

Regression Based Analysis of Strain Softening in Triaxial response of Indian coal ashes using Hyperbolic Model

Sajan Malviya¹ and Prishati Raychowdhury²

¹ Research Scholar, Indian Institute of Technology Kanpur, Kanpur, Uttar Pradesh, India.

² Associate Professor, Indian Institute of Technology Kanpur, Kanpur, Uttar Pradesh, India.

Abstract. India is primarily dependent on thermal power plants for its energy needs. Large quantities of coal ashes emanate as a by-product in this process. Coal ashes produced in form of bottom ash and fly ash are often mixed with large quantities of water for wet disposal and sluiced to on-site ash ponds. Recently, considerable emphasis has been laid on suitable utilization of coal ashes in various infrastructure development projects. However, prior to any application their behavior, particularly, the shear strength characteristics under varied loading and drainage conditions needs to be carefully examined. In this study, a numerical model has been developed to analyze the post-peak strain softening behavior of coal ashes. A co-ordinate system transformation approach is employed based on the classical Duncan-Chang hyperbolic curve to model the softening behavior of undrained coal ashes. The validation of the model has been accomplished using triaxial data of six pond ash and four fly ash specimens randomly selected from various Indian power plants. Furthermore, a multi-variable regression analysis has also been carried out to develop empirical relationships between the model parameters and stress and strain values corresponding to peak and residual state, and confining pressure of the sample.

Keywords: Coal Ashes, Hyperbolic soil model, Undrained triaxial behavior, Strain-softening, Regression analysis.

1 Introduction

India's coal consumption is likely to witness a two-fold increase from 407 million tonnes oil equivalents (mtoe) in 2015 to 833 mtoe in 2035 to meet its energy demands (BP Energy Outlook 2018). To ensure wide utilization of industry-generated coal ashes (both fly ash and pond ash), it is necessary to have a constitutive model that can represent the material behaviour aptly. It is equally important that the parameters of the model can be determined with relative ease using available laboratory and *in-situ* tests. Several studies have used unconsolidated undrained triaxial tests to assess the shear strength characteristics of fly ash with or without additives and admixtures, as well as fly ash-soil mixtures (Das and Yudhbir 2005; Ghosh and Subbarao 2007; Kaniraj and Havanagi 1999; Kim et al. 2005). McLaren and DiGioia (1987) after investigating the direct shear tests and consolidated drained triaxial tests results of 51 fly ash samples, attributed their shear strength primarily to the internal friction. Several researchers focused on the factors affecting shear strength parameters of fly ash (Indraratna et al.

1991; Singh and Panda 1996; Datta 1998) In comparison to fly ash, literature available on shear behaviour of pond ash is limited (Jakka et. al 2010; Mohanty and Patra 2015; Singh and Sharan 2014).

There have been several attempts to incorporate softening-hardening behaviour in Duncan-Chang (D-C) model (Jia et. al. 2020; Wan et al. 2020; Wang and Cui 2012, Guo et. al 2012). Ahangar-Asr et al. (2013) presented a unified framework for constitutive modelling of the axial stress-volumetric strain behaviour of granular soils using an evolutionary polynomial regression technique. Studies that address strain-softening behaviour of coal ashes are very limited. Malviya and Raychowdhury (2022) proposed a modified Duncan Chang model that can simulate the strain softening behaviour of Indian coal ashes using a co-ordinate transform approach.

2 Methodology

2.1 Classical Model

The classical hyperbolic stress-strain model was developed by Kondner et al. (1963) and subsequently improved by Duncan and Chang (1970) for simulating the triaxial stress-strain behaviour of soil (Eq. 1).

$$\sigma_d = \frac{\varepsilon}{\frac{1}{E_i} + \frac{\sigma_d}{\sigma_{ult}}} \quad (1)$$

And the stress dependent tangent modulus is given by

$$E_t = E_i \left[1 - \frac{\sigma_d^2}{\sigma_{ult}^2} \right] \quad (2)$$

where, σ_d = stress difference or deviatoric stress

ε = axial strain

E_i = initial tangent modulus

σ_{ult} = ultimate stress difference

For determining the values of E_i and σ_{ult} , a graph is plotted between ε/σ_d and ε . The y intercept is $1/E_i$, while the slope of the line gives σ_{ult} .

2.2 Proposed Model

Malviya and Raychowdhury (2022) proposed a coordinate transformation approach to simulate softening, which is discussed in brief here. Consider a coordinate system (σ_d' - ε') formed by rotating (σ_d - ε) in the clockwise direction and shifting the axis leftwards (in the negative direction) by a length of magnitude ε_0 such that the post-peak stress-strain curve in the original coordinate system follows the conventional hyperbolic model in the transformed coordinate system (σ_d' - ε') to the greatest possible accuracy. The relationship between deviatoric stress (σ_d') and axial strain (ε') in the transformed coordinate system can be expressed as:

$$\sigma_d' = \frac{\varepsilon'}{1 + \frac{\varepsilon'}{E_i' + \sigma_{ult}'}} \quad (3)$$

where, E_i' and σ_{ult}' are the initial tangent modulus and ultimate deviatoric stress of the hyperbolic curve used to simulate post-peak response in the transformed coordinate system, respectively. This equation can be rearranged into dimensionless form.

$$\frac{\sigma_d'}{\sigma_{ult}'} = \frac{\frac{\varepsilon' E_i'}{\sigma_{ult}'}}{1 + \frac{\varepsilon'}{\sigma_{ult}'}} \quad (4)$$

$$\sigma^{*'} = \frac{\varepsilon^{*'}}{1 + \varepsilon^{*'}} \quad (5)$$

where, $\varepsilon^{*'}$ and $\sigma^{*'}$ are transformed normalized strain and transformed normalized stress respectively.

$$\varepsilon^{*' } = \frac{\varepsilon' E_i'}{\sigma_{ult}'} \quad (6)$$

$$\sigma^{*' } = \frac{\sigma_d'}{\sigma_{ult}'} \quad (7)$$

Now, consider normalizing the original co-ordinate system using E_i' and σ_{ult}' exactly as is done in Eq. 4 & E. 5 to form a coordinate system $\sigma^* - \varepsilon^*$ with origin O . The normalization is shown in Eq. 8 & Eq. 9.

$$\varepsilon^* = \frac{\varepsilon E_i'}{\sigma_{ult}'} \quad (8)$$

$$\sigma^* = \frac{\sigma_d'}{\sigma_{ult}'} \quad (9)$$

If this coordinate system is rotated by an angle θ in the clockwise direction and the origin is shifted by ε_0^* towards negative x direction, the resulting system ($\sigma^{*' } - \varepsilon^{*' }$) with origin at O' would be exactly the same as described by Eq.4 and Eq.5. (Fig.1)

$$\varepsilon_0^* = \frac{\varepsilon_0 E_i'}{\sigma_{ult}'} \quad (10)$$

Using coordinate transformation Eq. 5 can be expressed in the $\sigma^* - \varepsilon^*$ co-ordinate system as:

$$(\varepsilon^* + \varepsilon_0^*) \sin \theta + \sigma^* \cos \theta = \frac{(\varepsilon^* + \varepsilon_0^*) \cos \theta - \sigma^* \sin \theta}{1 + (\varepsilon^* + \varepsilon_0^*) \cos \theta - \sigma^* \sin \theta} \quad (11)$$

The equations can be further simplified by using the following substitutions.

$$\varepsilon^* + \varepsilon_0^* = A \cos \chi \quad (12)$$

$$\sigma^* = A \sin \chi \quad (13)$$

The terms χ and A are defined as:

$$\chi = \tan^{-1} \frac{\sigma^*}{\varepsilon^* + \varepsilon_0^*} \quad (14)$$

$$A = [(\varepsilon^* + \varepsilon_0^*)^2 + \sigma^{*2}]^{\frac{1}{2}} \quad (15)$$

Substituting the values from Eq. 19 and Eq. 20, Eq. 18 transforms into an expression analogous to dimensionless form of the original Duncan Chang hyperbolic model.

$$A \sin(\theta + \chi) = \frac{A \cos(\theta + \chi)}{1 + A \cos(\theta + \chi)} \quad (16)$$

Considering

$$\psi = \theta + \chi \quad (17)$$

Eq. 23 can be rewritten as

$$A \sin \psi = \frac{A \cos \psi}{1 + A \cos \psi} \quad (18)$$

Differentiating Eq. 18 with respect to ε , gives the following expression for tangent modulus.

$$E_t = E_i' \left[\frac{\cos \theta - \sin \theta - (\varepsilon^* + \varepsilon_0^*) \sin 2\theta - \sigma^* \cos 2\theta}{\cos \theta + \sin \theta + (\varepsilon^* + \varepsilon_0^*) \cos 2\theta - \sigma^* \sin 2\theta} \right] \quad (19)$$

Physical Significance. The length of the line segment (O'P) joining the new origin to any point P on the post-peak curve in normalized co-ordinate system is the value of A for that point. The angle this line forms with ε^* axis is the value of χ for that

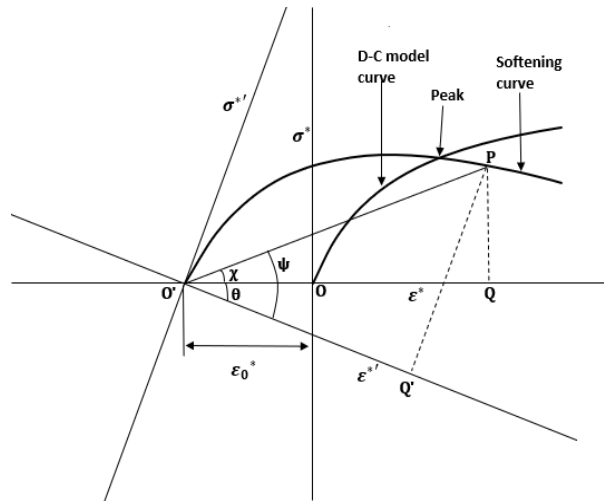


Fig.1. Representation of the curves for pre-peak and post-peak response.

point ($\angle PO'Q$, Fig.1). Further, ψ is the angle that line joining the new origin to any point on the post-peak curve forms with ε^* axis ($\angle PO'Q'$, Fig. 1). Thus $\tan \psi$ is effectively the secant modulus for the point on the curve corresponding to value ψ in the σ^* - ε^* coordinate system.

2.3 Simplified Model

The model can be considered to be a degenerated version of the earlier proposed model where ε_0 and θ are equal to zero. This simplified model uses two separate set of values of initial tangent modulus and ultimate stress values for pre-peak and post peak

response. This is similar to the composite two-segment hyperbolic (CTH) model used by Guo et. al (2012). However, in this model there is a negative value for initial tangent modulus for the post-peak curve. The pre-peak portion is analyzed exactly as in the proposed using Eq.1. For representing the post-peak curve, the following expression is used.

$$\sigma_d = \frac{\varepsilon}{\frac{1}{E_i''} + \frac{\varepsilon}{\sigma_{ult}''}} \quad \text{for } \varepsilon \geq \varepsilon_p \quad (20)$$

The values of E_i'' & σ_{ult}'' are determined by plotting the response obtained from the optimum fit curve using the proposed model (model 1) in the $\varepsilon/\sigma_d - \varepsilon$ plane. The y intercept is $1/E_i''$ while the slope of the line gives σ_{ult}'' .

3 Model Validation

3.1 Data Selection

The model has been developed for application in case of both, drained and undrained loading. But since, there is very limited literature available on drained triaxial tests for Indian coal ashes, only data available from undrained triaxial test results was analysed. The triaxial results were selected (Jakka et.al 2010, Patel 2013, Mohanty and Patra 2015) from the available literature in a random manner. Caution was exercised against any bias regarding specific gravity, OMC, degree of compaction, loading rate, confining pressure ranges, consolidation process and conditions during the selection. Six different samples of pond ash and four samples of fly ash, where softening can be observed, were chosen for the analysis. The details of physical properties and the source of origin can be found in the literature (mentioned above).

3.2 Parameter Optimization

The values of six parameters (E_i , σ_{ult} , θ , ε_0 , E_i' , σ_{ult}') are required for simulating a triaxial response for a given confining pressure for the proposed model. It was observed that it is possible to determine the parameters through graphical optimization using an iterative scheme.

Firstly, the pre-peak triaxial test data is analysed using the conventional approach. Subsequently, the post -peak data, isolated from a stress- strain triaxial data is considered for analysis. A spreadsheet macro was generated that employs the Goal Seek function in Excel for simultaneous operation for several data points. Stress responses are generated for given strain values using Eq. 11 to obtain the best fit curve. The sequence adopted in determining the model parameters for the post-peak response is mentioned below.

1. ε_0 is varied from 0 to ε_r .
2. θ is varied between 0 to 45 degrees.
3. E_i' and σ_{ult}' are subsequently optimized.

Important trends that emerged after a rigorous analysis are:

1. A very good fit can be obtained by choosing ε_0 value as $\varepsilon_r/2$.
2. The slope of the line joining the peak and final values in the $\sigma^* - \varepsilon^*$ coordinate system is the best initial approximation for the value of $\tan \theta$. An initial trial value equal to E_i can be considered for E_i' .

3.3 Optimization Results

The model parameters for presented in Table 1. Selected results have been depicted in Fig. 2, comparing the results predicted by the models and the test data. It is evident that the results of the proposed model are in good agreement with actual results. The salient features of the result of this analysis are presented here:

- [1] E_i and E_i' value increases with increase in confining pressure, density and relative compaction for a given coal ash. E_i values are slightly higher for coarser samples.
- [2] Since the initial tangent modulus for post-peak response E_i'' has a negative sign, the trend for $-E_i''$ is similar to E_i' values.
- [3] The ultimate deviatoric stress values corresponding to pre-peak portion, model 1 and model 2 that is σ_{ult} , σ_{ult}' and σ_{ult}'' respectively increase with increase in confining pressure for a given ash.

3.4 Determination of Model Parameters using Regression Analysis

An attempt was carried out to generate empirical relations between the model parameters and the observed test data using regression analysis. This exercise was accomplished with the aid of MATLAB curve fitting toolbox. A MATLAB code has been developed with the parameters obtained from earlier optimization along with the significant test data (confining pressure, stress and strain values corresponding to peak and residual state respectively) as input values. Variables are introduced in dimensionless form to assess their impact on model parameters. Each model parameter (in a dimensionless form) is evaluated as a polynomial function of one or more of these variables. The equations corresponding to the best fit curves are further used to compute another set of model parameter in the code. The model parameters generated using this regression analysis are employed to simulate a stress response for a specified strain vector depending on the test specifications of a given ash sample. These curves are called Regression generated (RG) curves.

Two distinct set of regression analysis models are developed for a comparative analysis. The first model (Regression model 1) is developed as a general model for the prediction of model parameters for both pond ash and fly ash samples, whereas the second model is specific to pond ash samples. This was done to investigate the possibility of a single regression model that can be used for all coal ashes.

Table 1. Optimized model parameters (Malviya and Raychowdhury 2022)

S. No.	Specimen	σ_3 kPa	Duncan Chang parameters		Proposed Model (Model 1)				Simplified Model (Model 2)	
			E_i (MPa)	σ_{ult} kPa	θ	ε_0	E_i' (MPa)	σ_{ult}' (kPa)	E_i'' (MPa)	σ_{ult}'' (kPa)
1		98.1	55.6	520	2	4	48.7	581	-28.6	286
2	Angul FA	196.2	60	1300	2	4.9	54.5	1060	-142.9	625
3		294.3	125	1400	2	4.7	80	1450	-200	833
4		98.1	47.6	526	10	1.7	52.7	980	-30.3	222
5	Talcher FA	196.2	48	1150	10	2.9	60	2150	-40	476
6		294.3	50	2200	6.5	2.5	120	2250	-62.5	625
7		98.1	37	555	10.2	1.8	60	1120	-17.5	189
8	Kaniha FA	196.2	38.5	975	4.8	2.9	80	1225	-24.4	357
9		294.3	40	1700	3	3.4	100	1430	-52.6	667
10		98.1	25	1300	3.5	3	62.5	930	-40	385
11	Kalunga FA	196.2	34	1300	5.5	3.5	60	1375	-34.5	435
12		294.3	38	1650	4	4	80	1775	-47.6	667
13		50	23	600	2	12.5	23	750	-10.2	345
14	Badarpur PA-1	100	25	720	2	12.5	25	850	-11.5	400
15		200	40	1050	2	12.5	43	1195	-14.1	500
16		100	27	1667	2	12.5	37.5	1675	-55.6	909
17	Badarpur PA-2	200	45	2500	3.3	12.5	50	2600	-29.4	1111
18		400	90	2600	4	12.5	90	3875	-14.9	909
19		100	4.25	1250	2	12.5	9	525	-32.3	323
20	Panki PA-1	200	9	1040	2	12.5	15	850	-45.5	526
21		300	16.9	1250	2	12.5	21	1345	-66.7	833
22		100	8.7	555	2	14	12.2	585	-10.9	313
23	Panki PA-2	200	18.9	714	2	14	19.5	945	-12.2	476
24		300	24.4	1200	2	14	24.5	1475	-27.8	833
25		100	5.3	450	2	12.5	11	450	-6.3	222
26	Panipat PA-1	200	6	900	2	12.5	20	815	-9.6	400
27		300	10	1020	2	12.5	30	1175	-12	588
28		100	4.8	460	2	14	12.8	491	-4.5	217
29	Panipat PA-2	200	7.8	769	2	14	20	875	-8.5	417
30		300	13.4	990	2	14	27	1250	-11.6	588

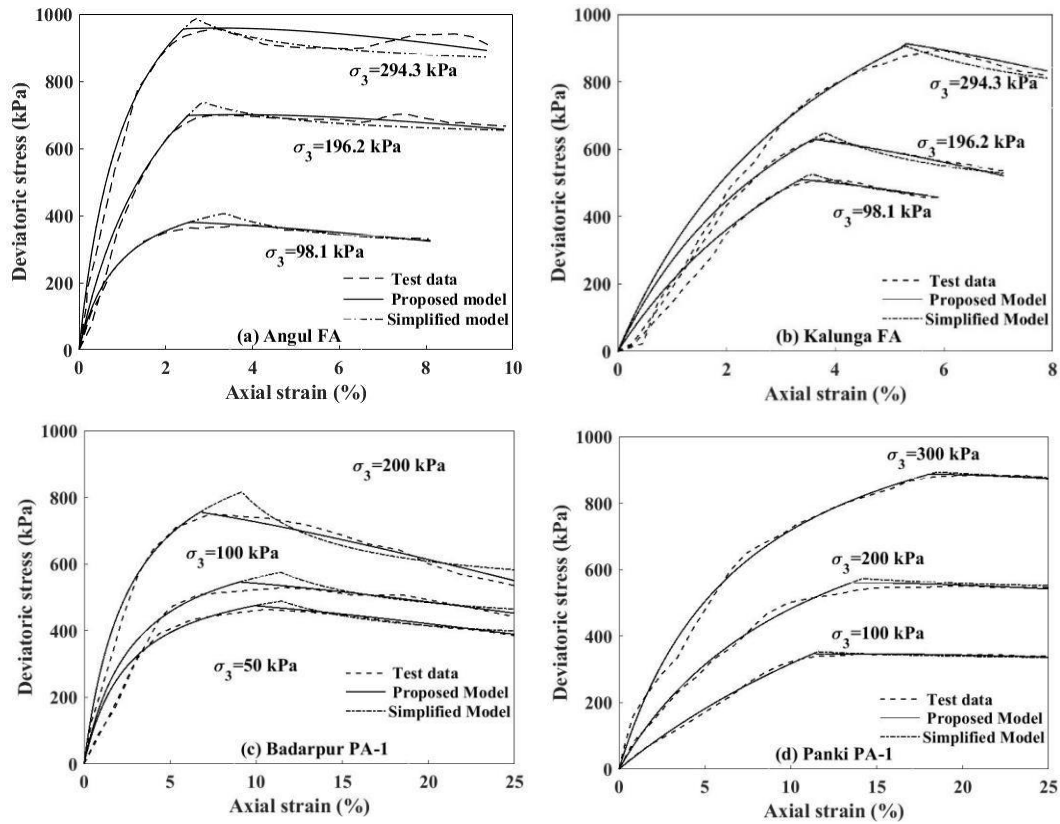


Fig.2. Comparison of proposed model and simplified model with the observed triaxial test results.

The model parameters for Angul FA, Talcher FA, Kalunga FA, Kaniha FA, Badarpur PA-1 and Badarpur PA-2 were estimated using first model (Table 2). The second model (Regression model 2) was used for Panki PA-1, Panki PA-2, Panipat PA-1 and Panipat PA-2 (Table 3). During regression analysis, it was observed that some of the model parameters (dependent) could not be evaluated directly from the test data. Their determination also required values of other model parameters (independent). The response generated from the predicted model parameters, required for the proposed model is defined here as the Regression Generated Proposed Model (RGPM), whereas the response generated from the predicted model parameters for the simplified model is defined as Regression Generated Simplified Model (RGSM). These curves are compared with the observed triaxial test data, and presented in Fig. 3 and Fig. 4. It can be observed that both RGPM and RGSM models perform reasonably well in simulating the triaxial test data in terms of peak values, initial and post-yield behavior and overall trend of the curves.

Table 2. Input variables used for Regression model 1.

S. No.	Parameter	Dimensionless form	Variable 1	Variable 2	Poly-nomial order	Adj. R ²	RMSE	SSE
1	E_i	$(\frac{E_i}{p_A})^2$	$(\frac{\sigma_3}{p_A})^2$	$(\frac{\sigma_{dp}}{\varepsilon_p p_A})^2$	33	0.95	7.895	498.63
2	σ_{ult} (dependent)	$\frac{\sigma_{ult}}{p_A}$	$\frac{\varepsilon_p E_i}{p_A}$	$\frac{\varepsilon_p E_i}{\sigma_{dp}}$	13	0.95	1.425	22.34
3	θ	$\tan \theta$	$(\frac{\sigma_3}{p_A})^2$	$(\frac{\sigma_d - \sigma_{dr}}{(\varepsilon_p - \varepsilon_r)p_A})^2$	15	0.99	0.004	9.5×10^{-5}
4	E_i'	$(\frac{E_i'}{p_A})^2$	$(\frac{\sigma_3}{p_A})^2$	$(\frac{\sigma_{dr}}{(\varepsilon_p - \varepsilon_r)p_A})^2$	33	0.97	6.184	305.97
5	σ_{ult}' (dependent)	$\frac{\sigma_{ult}'}{p_A}$	$\frac{\varepsilon_0 E_i}{p_A}$	$\frac{\sigma_{dr} \tan \theta}{p_A}$	11	0.98	0.894	11.98
6	σ_{ult}''	$\frac{\sigma_{ult}''}{p_A}$	$\frac{\sigma_{dr}}{p_A}$	-	1	0.98	0.397	2.52
7	E_i'' (dependent)	$(\frac{E_i''}{p_A})^2$	$(\frac{\sigma_{dr}}{\varepsilon_f p_A})^2$	$(\frac{\sigma_{ult}''}{p_A})^2$	34	0.99	8.168	266.87

* $\varepsilon_0 = \varepsilon_r/2$

4 Conclusions

A new approach has been developed to model the strain softening observed in triaxial test results. The model is a modification of the conventional Duncan Chang hyperbolic soil model using coordinate transformation. The approach is employed to simulate undrained triaxial test response for coal ashes. The model introduces four parameters to map the post-peak response. The model successfully reproduces the stress strain response once the parameters are optimized. The model can be degenerated to a simplified form where only two parameters are required for modelling the softening response has also been proposed. The simplified model has a discontinuity at ε^* ($\varepsilon E_i''/\sigma_{ult}''$) equals -1. Fortuitously in this study the discontinuity had no impact as the axial strain corresponding to peak state was always greater than the strain values corresponding to the discontinuity. Hence the post-peak curve, for all practical purposes is continuous.

The proposed model can be applied for both consolidated as well as unconsolidated specimens with satisfactory levels of accuracy. The model can be easily incorporated in an FEM simulation using Eq. 11 and Eq. 19. This can be done by specifying a yield criterion and using a return stress-like algorithm with stepped loading. The model is capable of pre-failure softening as well. The regression analysis relates the parameters

required for simulating the stress-strain response to the values that can be directly observed and obtained from the undrained triaxial test data. It is observed that the Regression model 2 yields better results as compared to the Regression model 1. With a larger database at our disposal the regression model can be fine-tuned for a better prediction of the model parameters, while retaining the original framework and henceforth the stress-strain response. The regression model also establishes that when the value of strain corresponding to peak state is close to the strain at residual state, the conventional D-C model should be preferred.

Table 3. Input variables used for Regression model 2.

S. No.	Parameter	Dimensionless form	Variable 1	Variable 2	Poly-nomial order	Adj. R ²	RMSE	SSE
1	E_i	$(\frac{E_i}{p_A})^2$	$\frac{\varepsilon_p \sigma_3}{\sigma_p}$	$(\frac{\sigma_{dr}}{\varepsilon_r p_A})^2$	33	0.95	0.381	0.29
2	θ	$\frac{\sigma_f \tan \theta}{p_A}$	$(\frac{\sigma_3}{p_A})^2$	$(\frac{\sigma_{dp} - \sigma_{dr}}{(\varepsilon_p - \varepsilon_r)p_A})^2$	13	0.97	0.013	4.8x10 ⁻³⁵
3	σ_{ult} (dependent)	$\frac{\sigma_{ult}}{p_A}$	$\frac{\varepsilon_0 E_i}{p_A}$	$\frac{\sigma_{dr} \tan \theta}{p_A}$	15	0.95	1.42	0.13
4	E_i'	$(\frac{E_i'}{p_A})^2$	$(\frac{\sigma_3}{p_A})^2$	$(\frac{\sigma_{dr}}{\varepsilon_r p_A})^2$	33	0.98	0.301	0.19
5	σ_{ult}' (dependent)	$\frac{\sigma_{ult}'}{p_A}$	$\frac{\varepsilon_0 E_i'}{p_A}$	$\frac{\sigma_{dr} \tan \theta}{p_A}$	11	0.99	0.197	0.35
6	E_i''	$(\frac{E_i''}{p_A})^2$	$(\frac{\sigma_3}{p_A})^2$	$(\frac{\sigma_{dr}}{\varepsilon_r p_A})^2$	33	0.97	2.159	9.32
7	σ_{ult}''	$\frac{\sigma_{ult}''}{p_A}$	$\frac{\sigma_{dr}}{p_A}$	-	1	0.97	0.381	1.45

* $\varepsilon_0 = \varepsilon_r/2$

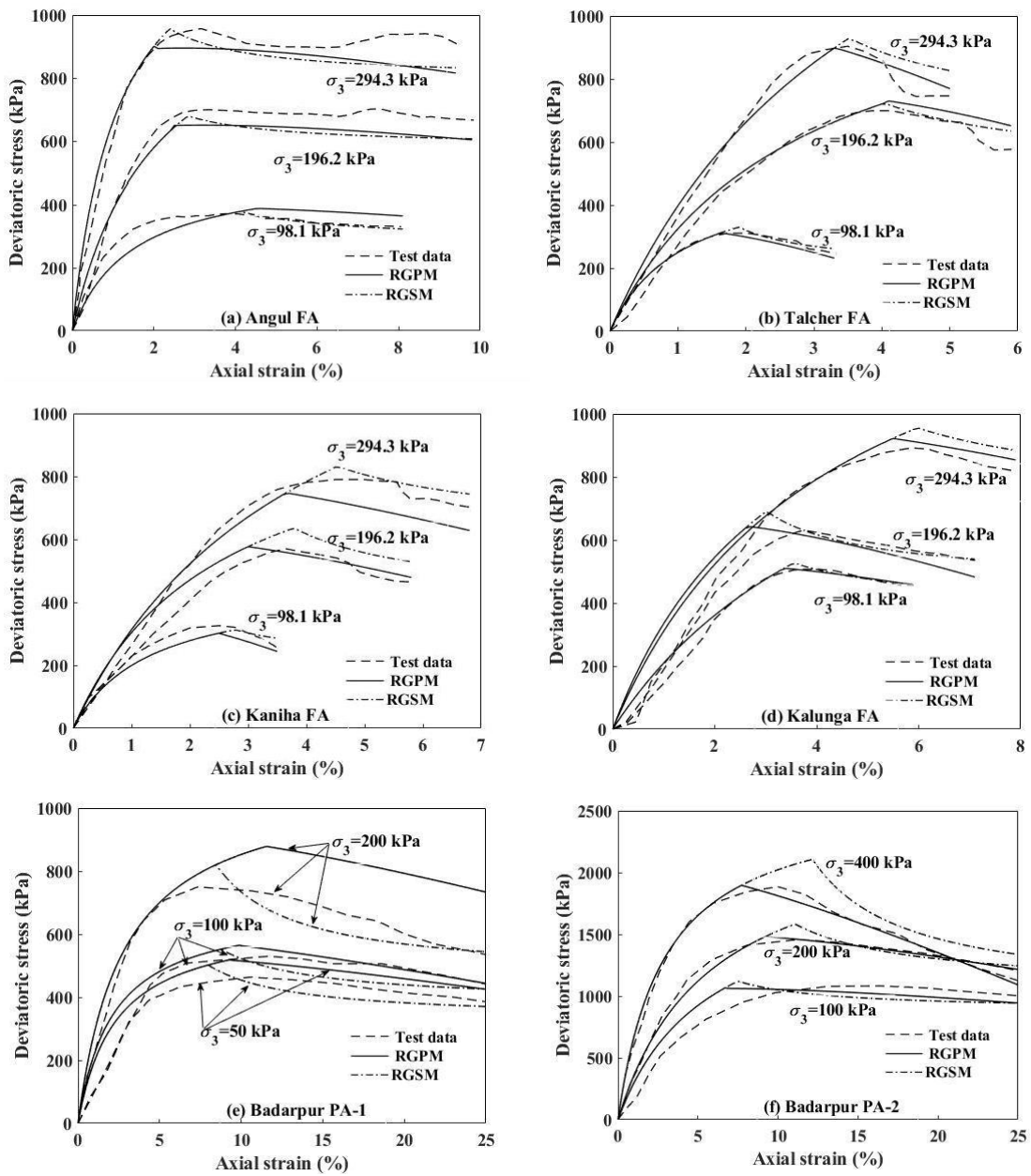


Fig.3. Comparison of Regression model 1 curves with the observed triaxial test data.

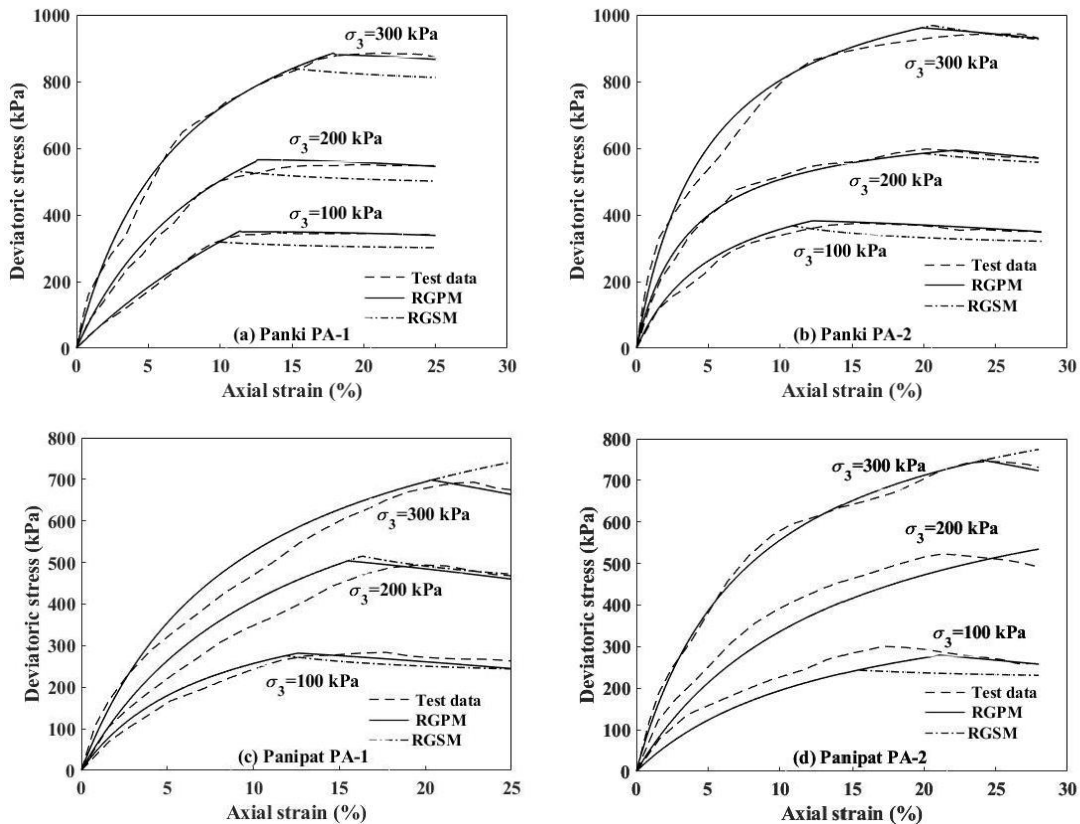


Fig.4. Comparison of Regression model 2 curves with the observed triaxial test data.

References

1. Ahangar-Asr, A., Faramarzi, A., Javadi, A. A.: Modelling stress-strain behaviour of granular soils. *Poromechanics V*, ASCE 2013, 1075-1081. <http://dx.doi.org/10.1061/9780784412992.128> (2013)
2. British Petroleum, BP Energy Outlook: 2018 Edition. Accessed 12 Aug 2018 (2018)
3. Das, S.K., Yudhbir, L. 2005.: Geotechnical characterization of some Indian fly ashes. *Journal of Materials in Civil Engineering*, 17(5):544–552. [https://doi.org/10.1061/\(ASCE\)0899-1561\(2005\)17:5\(544\)](https://doi.org/10.1061/(ASCE)0899-1561(2005)17:5(544)) (2005)
4. Datta, M. 1998.: Engineering properties of coal ash. In: *Proceedings of Indian geotechnical conference, Delhi, 2*, 41–46. (1998)
5. Duncan, J. M., Chang, C.Y.: Nonlinear analysis of stress and strain in soil. *Journal of Soil Mechanics and Foundations Division*, 32, 1629-1653. (1970)
6. Guo, J., Wang, W., Wang, X.: Improved Hyperbolic Model for Harden/soften Stress-strain Curve of Yangtze River Soil. *EJGE*, Vol. 17, Bund. L, 1675-1685. (2012)

7. Indraratna, B., Nutalaya, P., Koo, K. S. Kuganenthira, N. 1991.: Engineering behaviour of low carbon, pozzolanic fly ash and its potential as a construction fill. *Canadian Geotechnical Journal*, 28:542–555. <https://doi.org/10.1139/t91-070>. (1991)
8. Jakka, R. S., Ramana, G. V. Datta, M.: Shear behaviour of loose and compacted pond ash. *Geotechnical and Geological Engineering*, 28:763–778. <https://doi.org/10.1007/s10706-010-9337-1>. (2010)
9. Jia, P., Khoshghalb, A., Chen, C., Zhao, W., Dong, M., Esgandani, G.A. 2020.: Modified Duncan-Chang Constitutive Model for Modelling Supported Excavations in Granular Soils. *International Journal of Geomechanics*, 2020, 20(11): 04020211 [https://doi.org/10.1061/\(ASCE\)GM.1943-5622.0001848](https://doi.org/10.1061/(ASCE)GM.1943-5622.0001848). (2020)
10. Kaniraj, S. R., Havanagi, V. G.: Geotechnical characteristics of fly ash–soil mixtures.” *Geotechnical Engineering Journal*, 30(2):129–147. (1999)
11. Kim, B., Prezzi, M., Salgado, R. 2005.: Geotechnical properties of fly and bottom ash mixtures for use in highway embankments. *Journal of Geotechnical and Geoenvironmental Engineering*, ASCE, 131(7), 914–924. [https://doi.org/10.1061/\(ASCE\)1090-0241\(2005\)131:7\(914\)](https://doi.org/10.1061/(ASCE)1090-0241(2005)131:7(914)). (2005)
12. Kondner, R. L.: Hyperbolic stress-strain response: cohesive soils [J]. *Journal of the Soil Mechanics and Foundations Division*, ASCE, 1963, 89 (SM1): 115-143. (1963)
13. Malviya, S., Raychowdhury, P.: Analysis of strain softening for Indian coal ashes under Undrained Loading using Modified Duncan Chang model. *GeoTrans-2022*, Online International conference on Transportation Geotechnics, Jun 1-3, 2022, LBSITW, Thiruvananthapuram. (2022)
14. McLaren R. J., DiGioia, A. M.: The typical engineering properties of fly ash. In: *Geotechnical special publication no. 13*. ASCE, New York, 683–697. (1987)
15. Mohanty, S., N. R. Patra.: Geotechnical characterization of Panki and Panipat pond ash in India. *International Journal of Geo-Engineering* (2015) 6:13, Springer. <https://doi.org/10.1186/s40703-015-0013-4>. (2015)
16. Patel, A.: Characterization and classification of some local fly ashes.: MTech thesis, NIT Rourkela. <http://ethesis.nitrkl.ac.in/4744/1/211CE1230.pdf>. (2013)
17. Singh, S.P., Panda, A.P.: Utilisation of fly ash in geotechnical construction. In: *Proceedings of the Indian geotechnical conference, Madras, India*, 1, 547–550. (1996)
18. Singh, S.P., Sharan, A.: Strength characteristics of compacted pond ash, *Geomechanics and Geoengineering*, 9:1, 9- 17, DOI: 10.1080/17486025.2013.772661. (2014)
19. Wan, Z., Song, C., Gao, W.: Elastoplastic Model of Sand Based on Double-State Parameters under Complex Loading Conditions. *International Journal of Geomechanics*, 21(2): 04020256,1-29. [https://doi.org/10.1061/\(ASCE\)GM.1943-5622.0001915](https://doi.org/10.1061/(ASCE)GM.1943-5622.0001915). (2020)
20. Wang, H., Cui, T.: Softening amelioration of Duncan-Chang E-B model based on FLAC3D. *COTA International Conference of Transportation Professionals*, ASCE 2012. <https://doi.org/10.1061/9780784412442.330>. (2012)